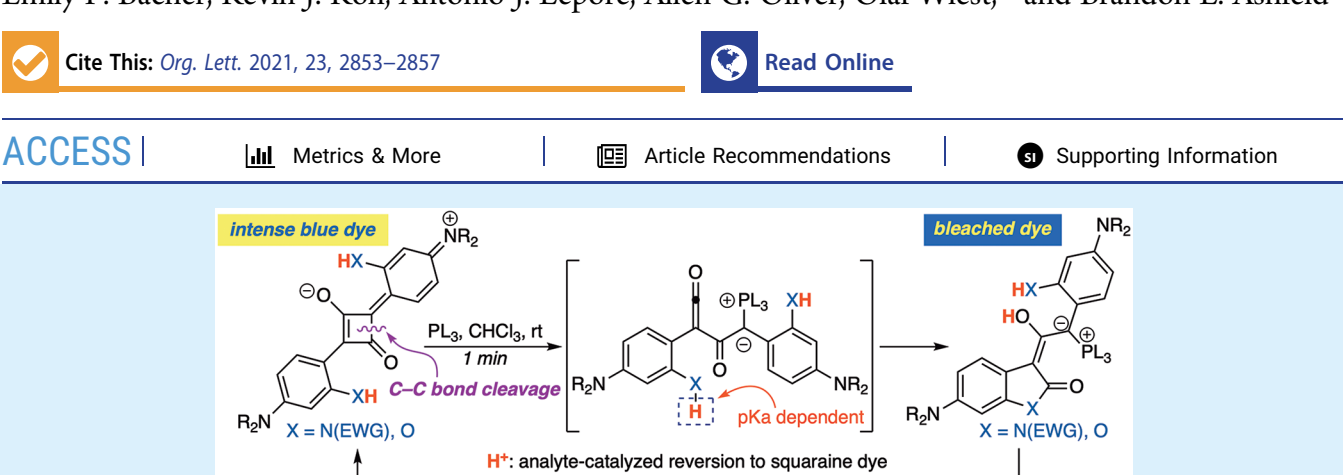


pubs.acs.org/OrgLett Letter

A Phosphine-Mediated Dearomative Skeletal Rearrangement of Dianiline Squaraine Dyes

Emily P. Bacher, Kevin J. Koh, Antonio J. Lepore, Allen G. Oliver, Olaf Wiest,* and Brandon L. Ashfeld*



ABSTRACT: A phosphorus(III)-mediated dearomatization of *ortho*-substituted dianiline squaraine dyes results in an unusual skeletal rearrangement to provide exotic, highly conjugated benzofuranone and oxindole scaffolds bearing a C3 side chain comprised of a linear conflagration of an enol, a phosphorus ylide, and 2,4-disubstituted aniline. Employing experimental and computational analysis, a mechanistic evaluation revealed a striking dependence on the acidity of the aniline *ortho* substituent. Notably, the rearrangement adducts underwent rapid and complete reversion to the parent squaraine in the presence of a Brønsted acid.

hemical dearomatizations have evolved into a powerful strategy for the construction of more complex, saturated synthetic building blocks from readily available starting materials. While most arene dearomatizations enable the installation of high-value functionalities that retain the core carbon framework, the initiation of a ring fragmentation cascade to assemble architecturally distinct scaffolds is substantially less common. A rare example of this was recently reported by Glorius and co-workers, who exploited visible light photocatalysis employing an IrIII photosensitizer to initiate a dearomative [2+2] cycloaddition of 2-naphthol derivatives to unveil a second photosensitive functionality.2 The subsequent energy transfer process resulted in a core skeletal reorganization of the starting naphthol framework to provide a cyclobutylarene (Figure 1a). Recently, we reported a reversible addition of phosphorus(III) reagents to dearomatize dianiline squaraine dyes 1 as chemodosimeters for transition metal complex detection, 3a in which the resulting thermo- and chemoreversible dynamic equilibrium resulted in a metaldependent spectroscopic response (Figure 1b).3 Over the course of this study, we speculated that upon dearomatization, the increased level of polarization renders the indicated squaraine C-C bond labile, and thus prone to spontaneous and reversible heterolytic cleavage. The installation of a nucleophilic functionality proximal to the squaraine core would promote a skeletal reorganization leading to a new aromatic framework. Herein, we report a dearomative ring fragmentation of ortho-heteroatom-substituted dianiline squaraine dyes 3/4 to the exotic enol ylide scaffolds 5/6 under

exceptionally mild reaction conditions (Figure 1c). Experimental and computational evaluation of the reaction mechanism revealed that retroversion of this unusual skeletal rearrangement readily occurs in the presence of a Brønsted acid, highlighting a peculiar pK_a dependence on incorporation of phosphine and providing a basis for chemodosimeter development.

Despite the potential for architectural diversification around a central cyclobutanedione core, the utility of squaraine dyes as synthetic building blocks constitutes an underdeveloped area in organic chemistry. Characterized by their absorption and emission of light in the near-infrared region (NIR), these highly conjugated compounds are widely utilized in physical and analytical chemistry,⁴ and their fluorescence and absorption properties have led to impressive advances in non-invasive imaging of biological structures and as sensitizers in photodynamic therapy.^{5,6}

The electrophilic character of the cyclobutenedione nucleus is frequently an impediment to the translational implementation of these dyes, which has led to macromolecular protection strategies to impede the addition of exogenous nucleophiles.⁷

Received: January 21, 2021 Published: March 26, 2021





X = O

6: X = NR

(a) Glorius (2018) - photocatalyzed dearomative ring fragmentation:

(b) Reversible squaraine dearomatization via nucleophilic phosphine addition:

Figure 1. Dearomative functionalizations. (a) Visible light-mediated, dearomative induced fragmentation of 2-naphthols. (b) Disruption of the squaraine aromaticity via the addition of $P^{\rm III}$. (c) Dearomatization-induced skeletal rearrangement of dianiline squaraines.

 PL_3 or L_nM-PL_3

H+ (cat.)

or ML

3: X = O

4: X = NR

HX

In contrast, we sought to exploit this electrophilicity to initiate a dearomative, skeletal reorganization to provide functionalized benzofurans (X = O) and oxindoles (X = NR'). In contrast to our previous work, the addition of P^nBu_3 to o-hydroxy squaraine 3a resulted in complete bleaching within 5 min and the formation of benzofuranone 5a in 94% yield (Scheme 1). The polycyclic framework of 5a was confirmed by X-ray

Scheme 1. Dearomative Rearrangement of the Squaraine

$$\mathsf{Et_2N} \overset{\bigcirc}{\bigoplus} \mathsf{HO} \overset{\longrightarrow}{\bigoplus} \mathsf{HO} \overset{\bigcirc}{\bigoplus} \mathsf{HO} \overset{\longrightarrow}{\bigoplus} \mathsf{HO} \overset{\longrightarrow}{$$

crystallography, which revealed a number of intriguing architectural features specific to this class of compounds. The resulting adduct is characterized by a high degree of functionalization, as illustrated by the presence of a 1,3-dicarbonyl motif residing as its enol, a conjugated phosphorus ylide, and a benzofuranone core with specific C6-dialkylamino substitution. The ylide motif exhibits less double bond character than a standard phosphorus ylide as indicated by a

P-C bond length of 1.846 Å, and an apparent electrostatic attraction between the phosphonium cation and benzofuran carbonyl. It is noteworthy that the presumptive zwitterionic phosphonium adduct 7a was not observed as a co-product in this reaction.

To evaluate the architectural limitations of this dearomative rearrangement, we assessed the generality of this process across an array of *o*-hydroxy and *o*-amino dianiline squaraine dyes (Table 1). Treatment of 2-hydroxy squaraines 3b and 3c with

Table 1. Assembly of Benzofuranones 5 and Oxindoles 6^a

 $^{\rm a}P^{\rm n}Bu_3$ (0.11 mmol) was added to a suspension of 3/4 (0.1 mmol) in CHCl $_3$ (0.1 M) at 25 $^{\rm o}$ C. See the Supporting Information for detailed experimental procedures.

PⁿBu₃ at room temperature resulted in rapid conversion to the corresponding benzofuranones 5b and 5c bearing N₁Ndibenzyl and N,N-diphenyl substitution at the arene 4-position in >99% and 93% yields, respectively. However, the 4morpholine and 4-pyrrolidine squaraines gave benzofuranones 5d and 5e in diminished yields, presumably due to the insolubility of the parent squaraines. Addition of excess P"Bu₃ (>3 equiv) failed to ameliorate the issue. Exposure of the oamino-substituted squaraines 4 underwent ring fragmentation to provide the corresponding oxindoles 6. The 2-N-acyl and 2-N-sulfonyl derivatives gave oxindoles 6a-d in high yields (from 72% to >99%). In contrast, squaraines 6e-h bearing o-N-alkyl, -benzyl, -allyl, and -propargyl substitutions failed to provide the expected oxindoles. It is noteworthy that the squaraine dye was retained unaltered, indicating that the equilibrium favors the intact squaraine 4. Variations of the N-

alkyl groups at the *para* position did not impact the efficacy of oxindole formation as illustrated by *N*,*N*-diallylamine and *N*,*N*-dipropargylamine derivatives yielding oxindoles **6i** and **6j** in 78% and 94% yields, respectively. Likewise, the *N*-allyl-*N*-methyl and *N*-methyl-*N*-propargyl squaraines cleanly provided the corresponding oxindoles in quantitative yields.

Employing unsymmetrical dianiline squaraines 8 sets the stage for competitive ring fragmentation to incorporate either X or Y into the heterocyclic core (Table 2). To examine the

Table 2. Unsymmetrical Dianiline Squaraine Dyes^a

 $^aP^nBu_3$ (0.11 mmol) was added to a suspension of 3/4 (0.1 mmol) in CHCl $_3$ (0.1 M) at 25 $^\circ$ C. See the Supporting Information for detailed experimental procedures.

relative propensity of N- and O-substitution to undergo addition to the cyclobutenedione, we assembled unsymmetrical squaraine dyes 8a-f and subjected each to "Bu₃P in CHCl₃ at 25 °C. Treatment of those squaraine dyes bearing a single *ortho*-substituted aryl group (8a-d) led to the formation of the anticipated benzofurans 9a and 9b and oxindoles 9c and 9d in excellent yields (79–94%). Treatment of 2-hydroxy-2'-acylamino squaraine dye 8e led to the formation of benzofuran 9e via selective *o*-hydroxy-induced ring fragmentation in 94% yield. Rearrangement to N-acyl oxindole 9f in the presence of an *o*-NMeAc proceeded in quantitative yield wherein the presence of a labile N-H likely determines the product distribution. The ability to employ unsymmetrical dianiline squaraine dyes provides an opportunity for orthogonal functionalization.

Attempts to synthetically modify the products led to a notable resiliency given the multitude of functionality present. Exposure of oxindole ylide **6a** to an array of carbon electrophiles (e.g., benzaldehyde, methyl iodide, allyl bromide, etc.) did not provide the anticipated C- or O-alkylation products at the ylide carbon, 3-oxindole position, enol or oxindole carbonyl. Intrigued by the unexpected robustness of these typically reactive functional groups, we probed the behavior of these Brønsted basic motifs in the presence of acid by exposure of oxindole **6a** to *p*-tolylsulfonic acid. Surprisingly, we discovered that rather than products resulting from direct protonation, within minutes reversion back to squaraine dye **4a** occurred in quantitative yield (Scheme 2). In combination with the inherent stability of adducts **5** and **6**, the ability to

Scheme 2. Acid-Promoted Reversion to the Parent Squaraine

regenerate the parent dye under mild and specific conditions has significant implications to sensing applications.

To gain insight into this unusual oxindole ylide reactivity profile, the mechanism for its formation, and the lack of reactivity observed with 4e-h, we performed a series of computational studies at the B3LYP+D3/6-311+G**+CPCM-(CHCl₃) level of theory using Gaussian16. The electrostatic potential across the framework of oxindole 6a reveals extensive delocalization of charge density across the extended π -system (Figure 2). As a result, the ylide anion is highly stabilized with

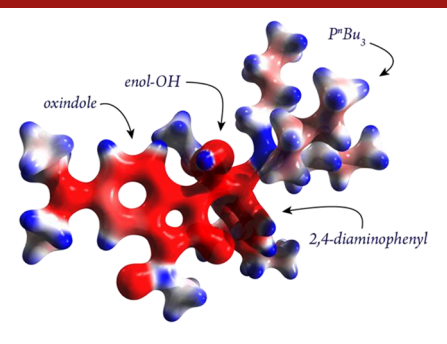


Figure 2. Electrostatic potential surface of 6a.

the p K_a of its conjugate acid estimated to be 9.17.¹⁰ This provides a rationale for the observed lack of ylide reactivity with a variety of electrophiles. It is also consistent with the X-ray crystal structure analysis of **5a** and **6a** showing a fully conjugated, extended π -system that includes the anionic carbon of the phosphorus ylide.

To elucidate the mechanism for the conversion of 3/4 to 5/ 6, we began with the assumption that formation of the phosphine adduct 7/10 precedes ring fragmentation given the rapid addition of PL₃ to squaraines we observed in the development of squaraine-based chemodosimeters (Scheme 3a).^{3a} As it relates to the formation of oxindole **6a**, three possible pathways can be envisioned to form 11a, which would then undergo a final proton transfer to form 6a: (i) ring closure to form tricyclic species 13, which would then undergo a ring opening event, (ii) a concerted pathway that proceeds via TS1, or (iii) an initial ring opening to form α -ketoketene 12a followed by nucleophilic attack of the amide nitrogen on the ketene sp carbon (Scheme 3b). Any attempts to optimize the geometry of 11a resulted in spontaneous formation of 6a. Similarly, the structures of 13a or TS1 could not be located and consistently resulted in the formation of 6a, suggesting that the nucleophilic addition pathway is not feasible and the reaction proceeds via the initial ring fragmentation to provide intermediate ketene 12a.

The Gibbs free energy diagram shows the computed pathways for the formation of $\mathbf{6a}$ (R = Ac; black), which proceeds in quantitative yield, and $\mathbf{6e}$ (R = Me; blue) where

Scheme 3. Mechanistic Considerations

(a) proposed mechanistic overview: ⊕_{NEt₂} AcHN NEt₂ PⁿBu_s ring migration NHAc NHAc NEt₂ NEt₂ Et₂N 4a 10a AcHN AcHN \bigcirc (proton transfer ⁿBu₃

(b) possible intermediates/transition states for conversion of **10a** to **6a**: ring fragmentation: nucleophilic addition:

Achn
$$\bigoplus_{\text{O}} \bigoplus_{\text{P}} \bigcap_{\text{Bu}_3} \bigoplus_{\text{Et}_2 N} \bigcap_{\text{12a}} \bigoplus_{\text{I2a}} \bigcap_{\text{I3}} \bigcap_{\text{H}} \bigoplus_{\text{R}} \bigoplus_{\text{Et}_2 N} \bigcap_{\text{TS1}} \bigcap_{\text{H}} \bigcap_{\text{R}} \bigcap_{$$

product formation is not observed (Figure 3). The formation of 10a from 4a is exergonic by 3.9 kcal/mol. The ring

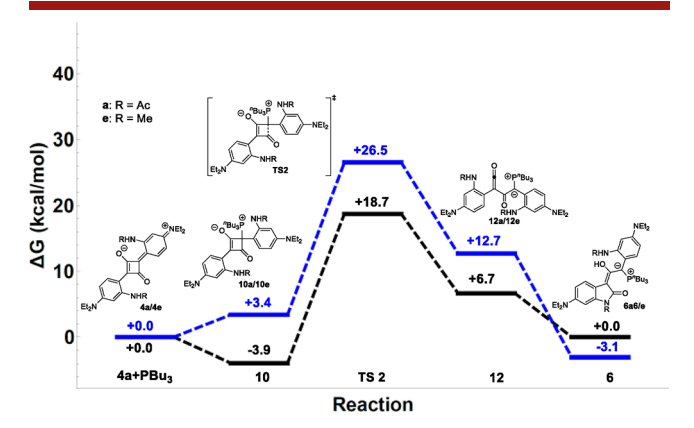


Figure 3. Potential free energy diagram for the formation of 6a/e from 4a/e (B3LYP+D3/6-311+G**+CPCM (CHCl₃)).

fragmentation via TS2 to form 12a occurs with an activation energy of 22.6 kcal/mol, which is consistent with a reaction occurring at room temperature on the hour time scale. Nucleophilic attack on the ketene followed by a proton transfer yields final product 6a in a reaction pathway that is overall thermoneutral.

A key difference in the reaction of **4e** is that the formation of the initial phosphonium adduct **10e** is endergonic by 3.4 kcal/mol, 7.3 kcal/mol less favorable than the formation of **10a**. Similar free energy differences between the two pathways are also obtained by **TS2** and **12**, but not in **6**. Consequently, the reaction of **4e** is not feasible at room temperature, in agreement with our experimental results. The similarity of the free energy difference along the pathway of the *N*-acyl and *N*-methyl derivative suggests the same origin for the energy difference in **10a/e**, **TS2**, and **11a/e**. The calculated structure of **10a** highlights key differences in H-bonds between the carbonyl and the NH moieties in **10a** and **10e** (Figure 4). The H-bonds are significantly elongated in **10e** compared to **10a**, which corresponds to the greater H-bonding ability of AcN—H

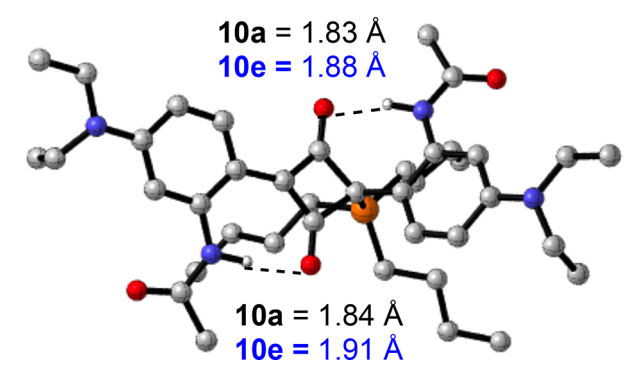


Figure 4. Structure of 10a (C-H bonds hidden for the sake of clarity).

relative to MeN-H. This effect is stronger after the addition of the phosphine, which leads to increased localization of the negative charge on the carbonyls, but disappears once the skeletal rearrangement to **6a/e** occurs.¹¹

As shown in Figure S1, scans of the N-C bond lengths in 12a show a barrierless transformation of 12a to 11a in agreement with the results discussed above. Similarly, a scan of the N-C bond in 11a leads to a barrierless N-deprotonation en route to 6a. These mechanistic steps are consistent with a classic general acid/base-catalyzed ring closure of 12a to 6a where the protonation/deprotonation step is coupled to N-C bond formation. It is well understood that such reactions cannot be accurately predicted by implicit solvent models or even a small number of solvent molecules. These results are consistent with the experimentally observed reversibility of the reaction upon treatment with a strong acid (Scheme 2). On the basis of the results shown in Figure 3, this step is thermoneutral but requires protonation of the weakly basic oxindole nitrogen, which is unlikely to occur spontaneously.

In conclusion, this study presents a versatile route by which ortho-substituted dianiline squaraine dyes serve as synthetic building block precursors to highly functionalized oxindoles and benzofurans through the addition of phosphines. Disruption of the aromatic core squaraine framework leads to a rapid and reversible dearomative ring fragmentation to produce a conjugated system bearing resilient enol and phosphonium ylide motifs in excellent yield. The surface electrostatic potential of this exotic scaffold revealed an extended conjugation that portends an unusual stability to a diverse array of stimuli. An exploration of the mechanism of this transformation revealed a dependency on the relative acidity of the proton residing on the ortho substituent of the starting dianiline squaraine dye whereby dearomative ring fragmentation leads to a proposed 1,2-ketoketene intermediate. Current studies are focused on the exploitation of this discovery in the context of target-directed alkaloid synthesis and a new class of chemodosimeters with wide-ranging potential for analyte detection.

ASSOCIATED CONTENT

Supporting Information

The Supporting Information is available free of charge at https://pubs.acs.org/doi/10.1021/acs.orglett.1c00248.

Experimental procedures, spectroscopic data, and crystallographic data (PDF)

Accession Codes

CCDC 2053259–2053260 contain the supplementary crystallographic data for this paper. These data can be obtained free of charge via www.ccdc.cam.ac.uk/data_request/cif, or by emailing data_request@ccdc.cam.ac.uk, or by contacting The Cambridge Crystallographic Data Centre, 12 Union Road, Cambridge CB2 1EZ, UK; fax: +44 1223 336033.

AUTHOR INFORMATION

Corresponding Authors

Brandon L. Ashfeld — Department of Chemistry and Biochemistry, University of Notre Dame, Notre Dame, Indiana 46556, United States; oorcid.org/0000-0002-4552-2705; Email: bashfeld@nd.edu

Olaf Wiest — Department of Chemistry and Biochemistry, University of Notre Dame, Notre Dame, Indiana 46556, United States; Oorcid.org/0000-0001-9316-7720; Email: owiest@nd.edu

Authors

Emily P. Bacher – Department of Chemistry and Biochemistry, University of Notre Dame, Notre Dame, Indiana 46556, United States

Kevin J. Koh — Department of Chemistry and Biochemistry, University of Notre Dame, Notre Dame, Indiana 46556, United States; © orcid.org/0000-0002-0412-4516

Antonio J. Lepore – Department of Chemistry and Biochemistry, University of Notre Dame, Notre Dame, Indiana 46556, United States

Allen G. Oliver – Department of Chemistry and Biochemistry, University of Notre Dame, Notre Dame, Indiana 46556, United States

Complete contact information is available at: https://pubs.acs.org/10.1021/acs.orglett.1c00248

Notes

The authors declare no competing financial interest.

■ ACKNOWLEDGMENTS

This work was supported by the National Science Foundation (CHE-1665440, 1956170, and 1855908). E.P.B. was supported by the CBBI Program and National Institutes of Health Training Grant T32GM075762.

■ REFERENCES

(1) (a) Pigge, F. C. Dearomatization Reactions. In Arene Chemistry; Mortier, J., Ed.; 2015; pp 399. (b) Wertjes, W. C.; Southgate, E. H.; Sarlah, D. Chem. Soc. Rev. 2018, 47, 7996. (c) Roche, S. P.; Porco, J. A., Jr. Angew. Chem., Int. Ed. 2011, 50, 4068. (d) López Ortiz, F.; Iglesias, M. J.; Fernández, I.; Andújar Sánchez, C. M.; Ruiz Gómez, G. Chem. Rev. 2007, 107, 1580. (e) Hoffmann, N. Photochem. Photobiol. Sci. 2012, 11, 1613. (f) Pettus, T. R. R.; Inoue, M.; Chen, X.-T.; Danishefsky, S. J. J. Am. Chem. Soc. 2000, 122, 6160. (g) Uyanik, M.; Ishihara, K. Asymmetric Oxidative Dearomatization Reaction. In Asymmetric Dearomatization Reactions; You, S. L., Ed.; 2016; pp 129. (h) Zhuo, C.-X.; Zhang, W.; You, S.-L. Angew. Chem., Int. Ed. 2012, 51, 12662. (i) Hudlicky, T.; Reed, J. W. Chem. Soc. Rev. 2009, 38, 2117

- (2) James, M. J.; Schwarz, J. L.; Strieth-Kalthoff, F.; Wibbeling, B.; Glorius, F. J. Am. Chem. Soc. 2018, 140, 8624.
- (3) (a) Bacher, E. P.; Lepore, A. J.; Pena-Romero, D.; Smith, B. D.; Ashfeld, B. L. Chem. Commun. 2019, 55, 3286. (b) Hewage, H. S.; Anslyn, E. V. J. Am. Chem. Soc. 2009, 131, 13099. (c) Houk, R. J. T.;

Wallace, K. J.; Hewage, H. S.; Anslyn, E. V. Tetrahedron 2008, 64, 8271.

- (4) Ajayaghosh, A. Acc. Chem. Res. 2005, 38, 449.
- (5) (a) Sreejith, S.; Joseph, J.; Lin, M.; Menon, N. V.; Borah, P.; Ng, H. J.; Loong, Y. X.; Kang, Y.; Yu, S. W.-K.; Zhao, Y. ACS Nano 2015, 9, 5695. (b) Harmatys, K. M.; Cole, E. L.; Smith, B. D. Mol. Pharmaceutics 2013, 10, 4263. (c) Cole, E. L.; Arunkumar, E.; Xiao, S.; Smith, B. A.; Smith, B. D. Org. Biomol. Chem. 2012, 10, 5769. (d) White, A. G.; Fu, N.; Leevy, W. M.; Lee, J.-J.; Blasco, M. A.; Smith, B. D. Bioconjugate Chem. 2010, 21, 1297. (e) Avirah, R. R.; Jayaram, D. T.; Adarsh, N.; Ramaiah, D. Org. Biomol. Chem. 2012, 10, 911.
- (6) (a) Prabhakar, C.; Bhanuprakash, K.; Rao, V. J.; Balamuralikrishna, M.; Rao, D. N. J. Phys. Chem. C 2010, 114, 6077. (b) Wang, S.; Hall, L.; Diev, V. V.; Haiges, R.; Wei, G.; Xiao, X.; Djurovich, P. I.; Forrest, S. R.; Thompson, M. E. Chem. Mater. 2011, 23, 4789. (c) Arunkumar, E.; Ajayaghosh, A.; Daub, J. J. Am. Chem. Soc. 2005, 127, 3156. (d) Gassensmith, J. J.; Matthys, S.; Lee, J.-J.; Wojcik, A.; Kamat, P. V.; Smith, B. D. Chem. Eur. J. 2010, 16, 2916. (7) (a) Arunkumar, E.; Forbes, C. C.; Noll, B. C.; Smith, B. D. J. Am. Chem. Soc. 2005, 127, 3288. (b) Arunkumar, E.; Fu, N.; Smith, B. D. Chem. Eur. J. 2006, 12, 4684.
- (8) Yang, M.; Jiang, Y. Phys. Chem. Chem. Phys. 2001, 3, 4213.
- (9) Frisch, M. J.; Trucks, G. W.; Schlegel, H. B.; Scuseria, G. E.; Robb, M. A.; Cheeseman, J. R.; Scalmani, G.; Barone, V.; Petersson, G. A.; Nakatsuji, H.; Li, X.; Caricato, M.; Marenich, A. V.; Bloino, J.; Janesko, B. G.; Gomperts, R.; Mennucci, B.; Hratchian, H. P.; Ortiz, J. V.; Izmaylov, A. F.; Sonnenberg, J. L.; Williams-Young, D.; Ding, F.; Lipparini, F.; Egidi, F.; Goings, J.; Peng, B.; Petrone, A.; Henderson, T.; Ranasinghe, D.; Zakrzewski, V. G.; Gao, J.; Rega, N.; Zheng, G.; Liang, W.; Hada, M.; Ehara, M.; Toyota, K.; Fukuda, R.; Hasegawa, J.; Ishida, M.; Nakajima, T.; Honda, Y.; Kitao, O.; Nakai, H.; Vreven, T.; Throssell, K.; Montgomery, J. A., Jr.; Peralta, J. E.; Ogliaro, F.; Bearpark, M. J.; Heyd, J. J.; Brothers, E. N.; Kudin, K. N.; Staroverov, V. N.; Keith, T. A.; Kobayashi, R.; Normand, J.; Raghavachari, K.; Rendell, A. P.; Burant, J. C.; Iyengar, S. S.; Tomasi, J.; Cossi, M.; Millam, J. M.; Klene, M.; Adamo, C.; Cammi, R.; Ochterski, J. W.; Martin, R. L.; Morokuma, K.; Farkas, O.; Foresman, J. B.; Fox, D. J. Gaussian 16, rev. C.01; Gaussian, Inc.: Wallingford, CT, 2016.
- (10) (a) Bochevarov, A. D.; Harder, E.; Hughes, T. F.; Greenwood, J. R.; Braden, D. A.; Philipp, D. M.; Rinaldo, D.; Halls, M. D.; Zhang, J.; Friesner, R. A. *Int. J. Quantum Chem.* **2013**, *113*, 2110. (b) *Jaguar pKa*, release 2019-4; Schrödinger, LLC: New York, 2019.
- (11) See the Supporting Information for further details.
- (12) (a) Jencks, W. P. Chem. Rev. 1972, 72, 705. (b) Dougherty, D. A.; Anslyn, E. V. Modern Physical Organic Chemistry; University Science: Sausalito, CA, 2006.
- (13) Plata, R. E.; Singleton, D. A. J. Am. Chem. Soc. 2015, 137, 3811.